New synthetic isochrones and predicted luminosity functions for stellar and substellar members of ω Centauri

Roman Gerasimov [1] Adam Burgasser [1] Derek Homeier [2] Jon Rees [3] Andrea Bellini [4] Luigi R. Bedin [5] Aaron Dotter [6] Mattia Libralato [4]

[1]University of California San Diego [2]Förderkreis Planetarium Göttingen [3]University of California Observatories / Lick Observatory [4]Space Telescope Science Institute [5]Istituto Nazionale di Astrofisica [6]Center for Astrophysics | Harvard & Smithsonian

Introduction

The coeval and co-evolving members of globular clusters serve as stellar astrophysics laboratories, as otherwise inaccessible parameters such as age and composition are often restricted within the cluster and may be inferred from its colour-magnitude diagrams. Until recently, the typically large distances of globular clusters confined such studies to their most massive members. Now, the promise of highly sensitive ground- and space-based facilities will extend the reach of these studies into the substellar regime.

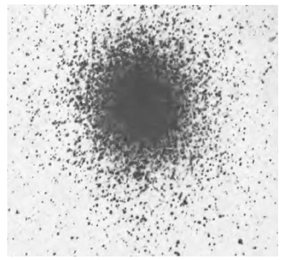

Figure 1: Allegedly [10] the earliest surviving photograph of ω Centauri by Sir David Gill, 1892. Reproduced from [8, p. 715].

We are investigating the elemental abundances of stars and the initial mass function (IMF) in one of the closest and most well-studied globular clusters, ω Centauri (Fig. 1), using a new grid of synthetic spectra and colour-magnitude diagrams. To our knowledge, these new models yield the best agreement with *HST* photometry. Comprehensive treatment of molecules and clouds enables us to make quantitative predictions for the properties of brown dwarfs in ω Centauri, which are expected to be observed for the first time in future studies with *JWST*, *TMT*, *GMT* and *ELT*.

Synthetic Isochrones

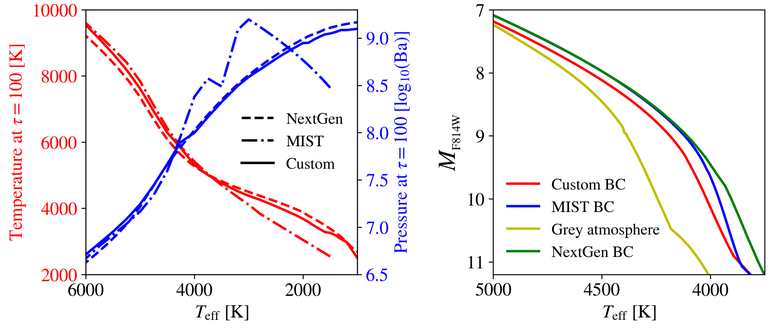

Figure 2: *Left:* boundary conditions for stellar structure at $\log(g) = 6.0$ and $[\mathrm{Fe/H}] = -1.4$. "*MIST*" refers to the set of boundary conditions used in `MIST` that are based on `ATLAS` atmospheres and become increasingly unreliable at low temperatures. "*NextGen*" conditions are derived using the grid of model atmospheres from [6, 2] that offers a better treatment of molecular opacities and convection but is less accurate than newer `PHOENIX` models due to the missing treatment of condensation and dust opacity as well as the use of scaled solar abundances. "*Custom*" boundary conditions are derived from our grid of atmospheres for the inferred abundances of ω Centauri (`A` in table 1). *Right:* the effect of the choice of boundary conditions on synthetic photometry of ω Centauri. Synthetic photometry derived under the assumption of grey atmosphere is shown for comparison. Note that the difference dissipates at high temperatures as expected. The magnitude displayed is *HST* WFC3 Vegamag.

We calculate new sets of evolutionary models and model atmospheres in the range $1\,\mathrm{kK} \leq T_{\rm eff} \leq 7\,\mathrm{kK}$. At high temperatures, we calculate model atmospheres with `ATLAS 9` [11, 12] for computational efficiency. Due to the incompleteness of the molecular opacity model, the accuracy of `ATLAS` degrades rapidly at $T_{\rm eff} \lesssim 4\,\mathrm{kK}$ where we use `PHOENIX 15` [1, 9, 5] instead. In addition to accounting for opacities due to $\sim 0.6 \times 10^9$ molecular transitions, `PHOENIX` allows 200 species to condense into dust under appropriate thermochemical conditions whose effect on both chemistry and opacity becomes increasingly important in brown dwarfs. Gravitational settling and convective mixing of dust are modelled using the Allard & Homeier cloud model [1, 7].

Stellar evolution up to 13.5 Gyr is modelled using the `MIST` framework [3, 15] with custom boundary conditions (temperature and pressure at $\tau = 100$) estimated by interpolating the atmosphere grid. The complexity of low temperature atmospheres leads to strong dependency of evolution on the chosen set of boundary conditions as illustrated in Fig. 2. Even at relatively warm effective temperatures ($\sim 4\,\mathrm{kK}$), synthetic photometry may be off by as much as a magnitude if the chosen set of boundary conditions fails to correctly model energy transport in the extended convection zones or enhancements of individual chemical elements. As such, isochrones available in literature fail to reach the substellar regime in globular clusters. Through the on-demand availability of model atmospheres with desired composition, this study is free of such limitation.

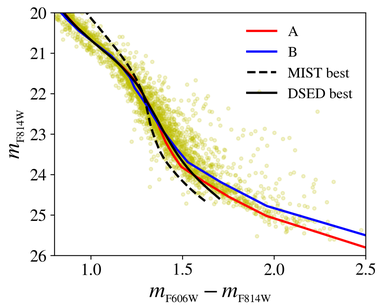

Figure 3: Two candidate isochrones (`A` and `B`) calculated in this study to approximate *HST* photometry of ω Centauri (in yellow). Closest matches from two model grids available in literature are also provided for comparison: `MIST` [3] and Dartmouth (`DSED`) [4]. The `MIST` isochrone is unable to model bright and faint members simultaneously. The Dartmouth isochrone performs considerably better but appears to have steeper than observed slope at the cold limit. Neither of the two literature isochrones extends far enough to cover the bottom of the main sequence or the substellar regime. All magnitudes and colours are *HST* WFC3 Vegamag.

	MIST	DSED	A	B
[Fe/H]	−1.70	−1.40	−1.40	−1.40
[α/Fe]	+0.00	+0.00	+0.40	+0.60
[C/Fe]	+0.00	+0.00	−0.65	−0.65
[N/Fe]	+0.00	+0.00	+1.45	+1.45
Y	0.25	0.40	0.40	0.40
Age	13.5 Gyr			

Table 1: Parameters of the isochrones shown in Fig. 3. The isochrones calculated in this study (`A` and `B`) only differ in [α/Fe] which appears to be sufficient to account for the scatter at the faint end of the main sequence. We therefore expect that the photometry of brown dwarfs in ω Centauri will strongly depend on abundances of individual elements. All isochrones are presented at the generously old age of 13.5 Gyr since the properties of the main sequence at low masses are approximately constant throughout the stellar lifetime which exceeds the age of the universe. Bracketed quantities are in dex compared to solar. Y is the helium mass fraction.

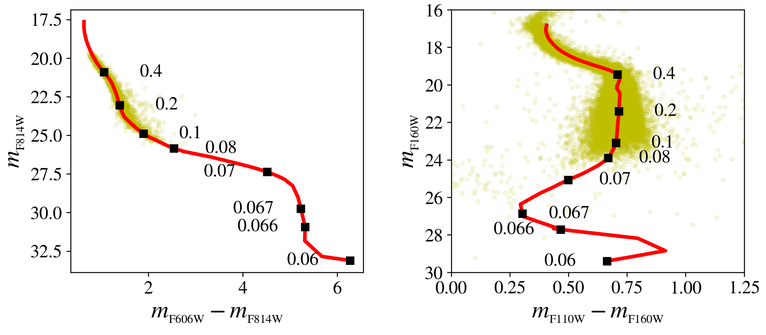

Figure 4: One of the candidate isochrones from Fig. 3, isochrone `A`, was extended down to $T_{\rm eff} = 1\,\mathrm{kK}$ into the substellar regime. *Left*: a zoomed out version of Fig. 3. *Right*: equivalent diagram in infrared bands. Numbers next to dark squares indicate stellar masses in $\mathrm{M}_\odot$. All magnitudes and colours are *HST* WFC3 Vegamag.

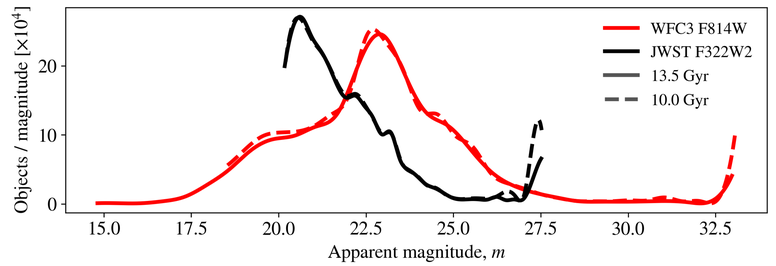

Figure 5: Predicted luminosity function for ω Centauri based on a best-fit broken power law IMF (see text) and the calculated isochrones. The emergence of the substellar population at the faint end and the brown dwarf gap are clearly seen. The distributions are normalized to the total mass of the cluster. All magnitudes are Vegamag.

The best-fit abundances of ω Centauri were calculated iteratively starting with initial guesses for [Fe/H], Y, [C/Fe], [N/Fe] and [O/Fe] based on photometric analysis in [14] and spectroscopy of individual bright stars from [13]. In each iteration, a synthetic isochrone was calculated and compared to optical *HST* photometry by evaluating the likelihood of the observed dataset, given the observed spread in colour around the fiducial (median) colour-magnitude relationship as a function of magnitude and the observed luminosity function (LF). We use the distance modulus of 13.6 from [17] and treat reddening as a free parameter. The assumed abundances were perturbed at the end of each iteration until a satisfactory fit to the data was obtained. The result of the fifth and final iteration is shown in Figs. 3 and 4 with comparison isochrones from literature [4, 3]. Neither of the literature isochrones shown supports enhancements of individual elements.

Initial mass function

We combine the inferred best-fit isochrone for ω Centauri with the commonly used broken power law IMF to predict the magnitudes and multiplicities of brown dwarfs in the cluster. At high masses ($> 0.5\mathrm{M}_\odot$), we assume the IMF to obey the standard $N \propto M^{-2.3}$ [16]. The low-mass power index was treated as a free parameter and determined by calculating the LF from the IMF and fitting it onto observed LF in optical *HST* photometry. The best-fit power index was calculated to be 0.69 ± 0.06. Finally, the inferred IMF was used to extend the observed LF into the substellar regime. The predicted LFs for *HST* WFC3/F814W and *JWST* F322W2 are plotted in Fig. 5. The emergence of brown dwarfs is seen at the cold end of the modelling range at $T_{\rm eff} \approx 1\,\mathrm{kK}$. Due to the low surface temperature, long wavelength observations with *JWST* allow the expected brightness of brown dwarfs to be increased by nearly 5 magnitudes and place it well within the expected limit of the telescope. The total number of predicted substellar objects strongly depends on the age of the cluster and may therefore be used to estimate it.

References

[1] F. Allard, D. Homeier, and B. Freytag. In: *Philosophical Transactions of the Royal Society of London Series A* 370.1968 (June 2012).
[2] F. Allard, P. H. Hauschildt, and A. Schweitzer. In: *The Astrophysical Journal* 539.1 (Aug. 2000).
[3] J. Choi et al. In: *The Astrophysical Journal* 823.2, 102 (2016).
[4] A. Dotter et al. In: *The Astrophysical Journals* 178.1 (Sept. 2008).
[5] R. Gerasimov et al. In: *Research Notes of the American Astronomical Society* 4.12, 214 (Dec. 2020).
[6] P. H. Hauschildt et al. In: 525.2 (Nov. 1999).
[7] C. Helling et al. In: *MNRAS* 391.4 (Dec. 2008).
[8] S. Hughes. *Catchers of the light: the forgotten lives of the men and women who first photographed the heavens: their true tales of adventure, adversity & triumph*. ArtDeCiel, 2013.
[9] T. O. Husser et al. In: *Astronomy & Astrophysics* 553, A6 (2013).
[10] S. Iovene. *Omega Centauri (NGC 5139) and Cirrus*. 2019.
[11] R. L. Kurucz. In: *SAO Special Report* 309 (1970).
[12] R. L. Kurucz. In: *Determination of Atmospheric Parameters of B-, A-, F- and G-Type Stars GeoPlanet: Earth and Planetary Sciences* (2014).
[13] A. F. Marino et al. In: *The Astrophysical Journal* 746.1, 14 (2012).
[14] A. P. Milone et al. In: *MNRAS* 469.1 (July 2017).
[15] B. Paxton et al. In: *The Astrophysical Journal Supplement Series* 192.1 (2010).
[16] A. Sollima, F. R. Ferraro, and M. Bellazzini. In: *MNRAS* 381.4 (Nov. 2007).
[17] J. Soltis, S. Casertano, and A. G. Riess. In: *The Astrophysical Journal* 908.1, L5 (Feb. 2021).